Non-contact Reflection Photoplethysmography towards Effective Human Physiological Monitoring

Ping Shi[1,2] Vicente Azorin Peris[1] Angelos Echiadis[1]

Jia Zheng[1] Yisheng Zhu[2] Peck Yeng Sharon Cheang[1] Sijung Hu[1,*]

[1]*Department of Electronic and Electrical Engineering, Loughborough University, Loughborough, Leicestershire LE11 3TU, UK*
[2]*Department of Biomedical Engineering, Shanghai Jiao Tong University, Shanghai 200240, China*

Received 20 Jul 2009; Accepted 12 Nov 2009

Abstract

A non-contact reflection photoplethysmography (NRPPG) with its engineering model was created to access human physiological information. The NRPPG engineering setup with a vertical cavity surface emitting laser (VCSEL) as a light source and a high-speed PiN photodiode as a photodetector was configured based upon the principles of light-tissue interaction and Beer-Lambert's law. In this paper, we present three aspects of the NRPPG performance: (1) photonics engineering work to capture photoplethysmographic signals with a non-contact manner in an optimal setup of the NRPPG; (2) a 5-minute protocol with 22 participants to determine a good agreement between NRPPG and contact photoplethysmography (CPPG) by means of Bland-Altman statistical analysis and Pearson's correlation coefficient; and (3) a physiological experiment designed for cardiac-physiological monitoring utilizing NRPPG. The experimental results suggest that clean PPG signal can be obtained between 30-110 mm. The outcome from agreement study indicates that the performance of NRPPG is compatible with CPPG. The NRPPG technique has great potential in cardiac-physiological assessment in a required clinical circumstance.

Keywords: Non-contact reflection photoplethysmography (NRPPG), Sensor placement, Bland-altman plot, Pearson's correlation, Cardio-physiological monitoring

1. Introduction

Photoplethysmography (PPG) is a non-invasive optical technique for measuring changes in blood volume based on variations in light intensity passing through, or reflected from, skin tissue using a light source and a photodetector [1]. The variation in the detected output is generated by the pulsation of arterial blood within the peripheral vasculature as stimulated by the quasi-periodic cardiac cycle [2]. The most recognized PPG waveform feature is the peripheral pulse, which is synchronized to each heartbeat. It is generally accepted that PPG signals can provide valuable cardiovascular information [3].

The basic form of PPG technology only requires two opto-electronic components: a light source to illuminate the tissue (e.g. skin), and a photodetector to measure the small variations in light intensity associated with changes in perfusion in the catchment volume. The use of conventional contact PPG (CPPG) probe, whereby the light source and the detector are in contact with the skin surface, limits measurements to tissue sites where the probe fits. Additionally, the CPPG probe cannot be used where mechanical isolation is required, for instance, skin-burned patients. Moreover, the PPG signals detected in a contact manner could be affected by the contact force between the PPG probe and the measurement site as the arterial geometry could be deformed by compression.

Non-contact PPG probe can be considered as an alternative to overcome the limitations when using CPPG probe. The non-contact PPG could be directly beneficial for neonates, patients with skin wounds in cardiovascular monitoring and for large-scale population screening with hygiene concern. Non-contact PPG was initially explored by the researchers at Loughborough University [4,5]. A contactless imaging PPG technique has also been developed recently [6,7] to map tissue blood perfusion and monitor microcirculation of a specific tissue area *in vitro*. For the latter technology, the expensive components, larger data capacity requirement and relative complexity in signal processing are likely to hinder its popularity in the context of patient monitoring. Yet, non-contact PPG could yield cost-effective biomedical monitoring, simple signal

* Corresponding author: Sijung Hu
Tel: +44-0-1509227058; Fax: +44-0-1509227108
E-mail: S.Hu@lboro.ac.uk

processing, and instant assessment. Motion artifact reduction for PPG has been already considered theoretically and implemented physically [4,8]. The direct coupling in non-contact PPG was studied in order to make the probe practicable to meet the requirement of biomedical monitoring [5]. With the recent growth of medical and biomedical environments, a practical non-contact PPG solution can fulfill this demand for clinical monitoring. There are two modes of PPG techniques: transmission mode and reflection mode. Transmission mode, where the light source is on one side of the tissue and the photodetector on the other, is limited to areas where the perfused tissue is relatively transparent and hence allows transmitted light to be detected through the tissue. Normally transmission probes are placed on the subject's finger, toe, earlobe or nose. Yet reflection mode, where light source and photodetector are positioned on the same side of the skin surface, allows measurement of backscattered light on the human body where the probe can be virtually placed.

The goal of this study was to develop a contactless measurement technique, namely non-contact reflection photoplethysmography (NRPPG), which can enable PPG signal captured from a remote distance. In this study, we illustrate a NRPPG photonics engineering setup and show the results from a comparison study between NRPPG and CPPG and from a physiological experiment. Furthermore the outcome of this study reveals the NRPPG's potential in physiological assessment.

2. Methods

2.1 Non-contact PPG model

A NRPPG model based upon the Beer-Lambert's law [9] was taken into account to describe the relationship between the light incident on a biological tissue and the light received after transmission through it. Beer-Lambert's law was adapted based upon the present measurement method, which relies on the varying light absorption due to arterial blood volume change during a cardiac cycle.

Figure 1 shows a simplified diagram of the light distribution of the NRPPG model. I_i is the light incident on the skin surface, I_0 is the intensity of light penetrating the skin, I_r is the reflected light intensity and I is the intensity of light emerging from the tissue through the banana effect [10].

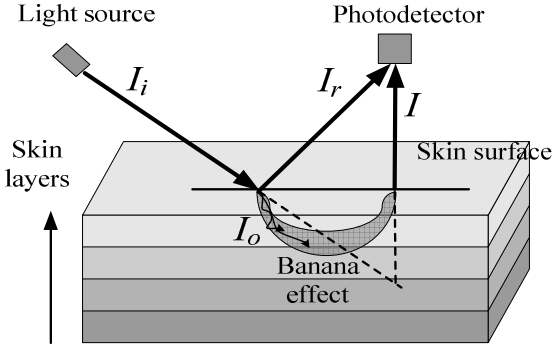

Figure 1. Simplified representation of light distribution.

The light reaching the photodetector can be separated into non-dynamic (DC) and dynamic (AC) terms [11]. *DC* consists of the reflected component (I_r) and the static component (from non-variable absorbers, i.e. tissue, bone, static blood, etc.), while *AC* represents the variation of light absorption due to arterial blood volume change. *I*, thus, can be expressed as:

$$I = I_o \exp(-\mu_{eff} r) = I_o \exp[-\mu_{dynamic} d(t) - \mu_{static} m] \quad (1)$$

where $\mu_{dynamic}$ is the extinction coefficient of the dynamic component, and μ_{static} is the extinction coefficient of static components. The light path length through the dynamic and static components are *d(t)* and *m*, respectively.

The primary target of this study was to calculate pulse rate variability (PRV) derived from PPG signals, in which the accuracy of PRV depends upon the quality of the *AC* term. Therefore the *dynamic (AC)* term should be maximized during the measurement period. This can be achieved by maximizing the light intensity that travels through the tissue *I*, while minimizing the reflection component of the static signal I_r in order to avoid saturating the photodetector. The light intensities at the illuminated surface and the detector are given by $I_i = I_o + I_r$ and $I_t = I_r + I$, respectively. The normalised *AC* term is directly proportional to I/I_r, and is maximized when I_r is minimized.

The light intensity at the detector can be expanded by applying the Taylor series first order approximation to the dynamic term for the exponential function ($e^{-x} = 1 - x$, $x \approx 0$):

$$\begin{aligned} I_t &= I_r + I_o \exp[-\mu_{dynamic} d(t) - \mu_{static} m] \\ &= I_r + I_o \exp(-\mu_{static} m)[1 - \mu_{dynamic} d(t)] \end{aligned} \quad (2)$$

From equation (2), the *static* term $I_r + I_o \exp(-\mu_{static} m)$ is the *DC* component of the detected signal obtained by low-passing the signal, e.g. 10th order Butterworth [12], $f_{cut\text{-}off}$: 0.3 Hz; and the *AC* component is $I_o \exp(-\mu_{static} m)\mu_{dynamic} d(t)$, which is obtained by band-passing the signal, e.g. 10th order Butterworth, f_1: 0.5 Hz, f_2: 5 Hz. The *AC* term becomes independent of the light source intensity by normalizing the *AC* with respect to the *DC*:

$$\frac{AC}{DC} = \frac{I_o \exp(-\mu_{static} m)\mu_{dynamic} d(t)}{I_o \exp(-\mu_{static} m)} = \mu_{dynamic} d(t) \quad (3)$$

Hence the amplitude of the normalized *AC* is proportional to the time-variant arterial light path length, which in turn depends on the characteristics of the banana shape. In practice, the reflected light is significant, resulting in an additive term in the denominator of equation (3), the minimization of which results in a maximized dynamic term.

2.2 Non-contact reflection PPG photonics engineering setup

For the hardware setup, a vertical cavity surface-emitting laser (VCSEL, Mode: PH85-F1P1S2, 10 mw, 850 nm, Roithner LaserTechnik Ltd, Austria) with an inherently narrow beam divergence of 30° and a high coherence was employed as a light source and was positioned to the illuminated tissue area at a changeable incident angle θ_{PL}. A high-speed silicon PiN photodiode (Model: S5821-03, Hamamatsu Photonics UK Ltd.,

England) with a high sensitivity over the spectral range of 500-1000 nm and the viewing angle of 10º was employed as a photodetector. The signals from the NRPPG engineering setup and a commercial CPPG probe (P861RA, 664 nm and 890 nm, Viamed Ltd., UK) were simultaneously captured by a 4-channel PPG board (DISCO4, Dialog Devices Ltd., UK). The analog-to-digital conversion for these captured PPG signals was implemented by a data acquisition board (USB-6009, National Instruments Co., USA), and the control software of the PPG board was performed by LabView 7.1 (National Instruments Co., USA) running on a Pentium IV computer.

The NRPPG photonics engineering setup was used to find an appropriate geometrical relationship between the positions of the light source and the photodetector. Directly coupled (reflected) light is dependent on the incident angle (θ_{PL}). Assuming a point source illumination and a fixed probing area in an empirical non-contact reflection measurement setup, the separation between the point of illumination and the probed area (l), which is determined by the incident angle (θ_{PL}) as well as the distance between the photodetector and the tissue (d_{PH}), determine the characteristics of the banana effect. The light source beam has a finite width in practice, therefore it is necessary to introduce an additional parameter for the separation between the light source and the photodetector (d_{PL}) which determines the characteristics of the illuminated surface. The focus plane of the illuminated tissue varied with the distance of the hand to the photodiode (d_{PH}). Figure 2 illustrates the relationship between these parameters.

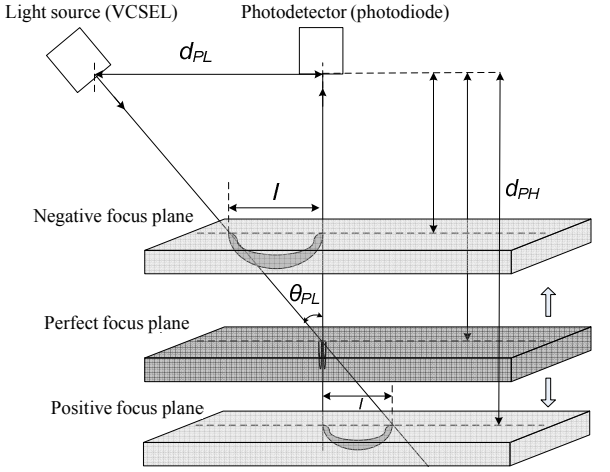

Figure 2. Instrumental hardware setup for NRPPG system illustrating the fundamental parameters. θ_{PL} and d_{PL} are the parameters that determine the position of the VCSEL and photodiode. By moving the hand closer to or further from the photodiode, the focus plane will change position accordingly.

The experimental process of optimization for the geometrical characteristics of the NRPPG system aimed to minimize the direct coupling by adjusting incident angle θ_{PL} while determining separation d_{PL} for optimum dynamic signal detection. The angle of the photodiode was fixed perpendicular to the tissue. The VCSEL was positioned at an incident angle (θ_{PL}) of 35°, 25° and 15° as well as a distance of the sensor placement against the photodiode (d_{PL}) at 15 mm, 25 mm and 35 mm, respectively.

2.3 PPG signals captured by NRPPG and CPPG

Twenty-two healthy subjects (M/F: 12/10, age: 29.0 ± 9.0 years, height: 1.70± 0.10 m, BMI: 23.1 ± 4.6 kg/m^2) participated in this study. Written informed consent was obtained from all volunteers prior to participation in accordance with the guidelines of the University Ethics Committee. The subjects were asked to breathe spontaneously. The PPG signals from NRPPG and CPPG system were recorded simultaneously from the right index fingertip and the right hand palm. Prior to the data processing, the ectopic beats from these PPG signals were filtered by using Matlab 7.0 (The MathWorks, Inc., USA). Four parameters, i.e. mean pulse-to-pulse intervals (PPI), standard deviation of consecutive PPI (SDPP), the width (SD1) and length (SD2) of Poincaré plot [13], were introduced to compare the performance between NRPPG and CPPG. These four variables provided the pulse rate duration (assessed by PPI), the PRV level (assessed by SDPP), the short-term PRV (assessed by SD1) and the long-term PRV (assessed by SD2). Pearson correlation coefficients r with respective p values were analysed in the linear association between the measurements of NRPPG and CPPG. Bland-Altman plots [14,15] were used for agreement analysis of the two measurement techniques, i.e. NRPPG and CPPG.

2.4 A physiological monitoring protocol

A physiological monitoring protocol was designed to investigate the nature of pulsatile variations using the NRPPG engineering setup. One female volunteer aged 27 and without known vascular disease participated in this study. The procedures of the protocol performance were in accordance with the approval of the University Ethics Committee. The PPG signals from the NRPPG setup was recorded in the morning and in the afternoon per day during the period of fourteen working days. The PPG signals were recorded for 3 minutes during each time at the same location of the left hand palm, where the peripheral arteries are close to the skin surface. The subject was asked to sit still and breathe normally during the detection.

A Butterworth low-pass filter was used to smooth the PPG signals recorded from the NRPPG. The heart rate series were then extracted offline by means of Matlab 7.0. A quantitative two-dimensional vector analysis of a Poincare plot was introduced to separately determine the standard deviation of instantaneous PRV (SD1), the standard deviation of continuous long-term PRV, (SD2) and their ratio (SD1/SD2). Poincaré plot analysis delivers a summary as well as the detailed beat-to-beat information on cardiac behaviour.

3. Results

3.1 Geometrical parameters for non-contact reflection PPG photonics engineering setup

Referring to the quality of opto-electronic signals, the detectable range of the distance between photodetector and hand (d_{PH}) was divided into three ranges: (1) the saturation range: the opto-electronic signal was captured but the

Table 1. The optimal distance range referring the opto-electronic signal's quality.

Configuration No.	*I*		*II*		*III*	
θ_{PL}(°); d_{PL}(mm)	*35; 15*		*25; 25*		*15; 35*	
	d_{PH}(mm)	l (mm)	d_{PH}(mm)	l (mm)	d_{PH}(mm)	l (mm)
Saturation range	< 30	< 6	< 30	< 11	< 40	< -24*
Optimal range	30 to50	6 to 20	30 to 110	11 to 26	40 to 90	-24 to 11
Low signal range	> 50	> 20	> 110	> 26	> 90	> 11

θ_{PL}: the angle of the VCSEL set against the photodiode.
d_{PL}: the distance between the VCSEL and the photodiode.
d_{PH}: the distance between the hand palm and the photodiode.
l: the banana shape distance between light entry and exit points.
*: the negative value referring to the position of hand palm at the negative focus plane.

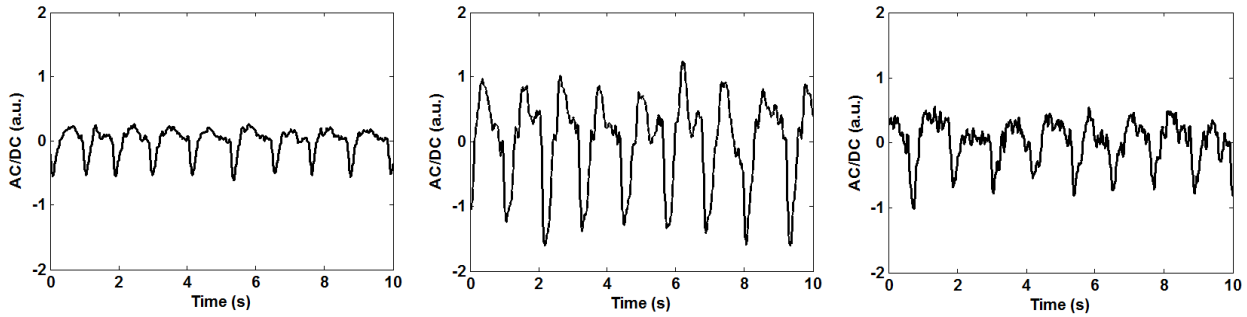

Figure 3. Representative PPG signals captured from NRPPG photonics engineering setup: (a) the saturation range, (b) the optimal range and (c) the low signal range, respectively.

photodetector became saturated easily in some cases; (2) the optimal range: a cleaner PPG signal was detected without any saturation of photodetector, and also the amplitude of the PPG signal varied with the change of the light source (VCSEL) output; and (3) the low signal range: the PPG signal was clearly detected with a bigger power of light source, and the PPG signal was sensitive to the interference of ambient light.

As shown in Table 1, by increasing the separation distance between the VCSEL and the photodiode from 15 mm to 35 mm and decreasing the incident angle from 15° to 35°, the variations of the three defined ranges were given experimentally. The projected light captured in the engineering setup was most likely to have travelled along a curved "banana-shaped" path through the tissue, thus, the banana shape distance between entry and exit points (l) in the three configurations was measured accordingly. Figure 3 presents the representative signals captured from the saturation range, the optimal range and the low signal range, respectively.

3.2 Comparison of PPG signals between NRPPG and CPPG

Figure 4 presents a synchronizing record of PPG signals detected by CPPG and NRPPG for 5 seconds from a representative subject. The feature of the PPG signals captured by NRPPG shows a similarity to that from CPPG. As presented in Table 2, the median values and the interquartile ranges describing the pulse rate parameters show the compatibility of the two techniques; the strong linear associations ($r \geq 0.97$) were found between two measurements of each parameter. Figure 5 shows the results of Bland-Altman analysis between the paired values of pulse rate parameters from CPPG and NRPPG. The good agreements are presented for Mean PPI (95% CI: -6.8 to 8.1 ms), SDPP (95% CI: -5.1 to 2.3 ms), SD1 (95% CI: -10 to 3.4 ms), and SD2 (95% CI: -3.2 to 1.9 ms).

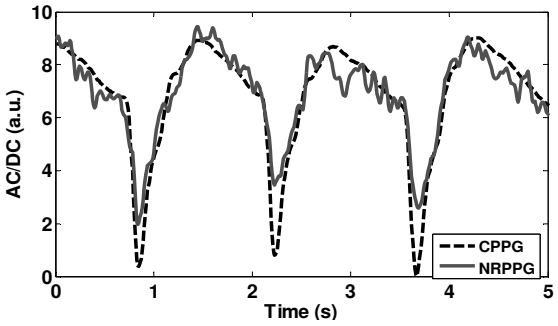

Figure 4. Comparison of CPPG and NRPPG signals.

Table 2. The comparison and correlation between CPPG and NRPPG for HR variables of Mean PPI, SDPP, SD1 and SD2.

Parameters	CPPG	NRPPG	correlation coefficients (r)	p
Mean PPI (ms)	842.3 (677.6-916.7)	843.1 (677.1-916.4)	0.99	0.42
SDPP (ms)	39.7 (25.8-60.9)	40.2 (30.8-62.2)	0.99	0.002
SD1 (ms)	21.1 (15.0-35.1)	26.4 (19.6-39.7)	0.97	0.0002
SD2 (ms)	52.5 (22.8-76.8)	52.5 (35.2-77.0)	0.99	0.03

3.3 Physiological monitoring

Figure 6 and Table 3 present the results from the designed physiological experiment utilizing NRPPG as described in Section 2.4. Significant increases for SD1 ($p = 0.0074$) and SD1/SD2 ($p = 0.001$) were found in the afternoon compared to those in the morning. No significant change was found for SD2 ($p = 0.1280$). Figure 7 presents the representative Poincaré plots of the test in the morning and in the afternoon on the same day. The physiological difference could be interpreted from the shape of the cloud.

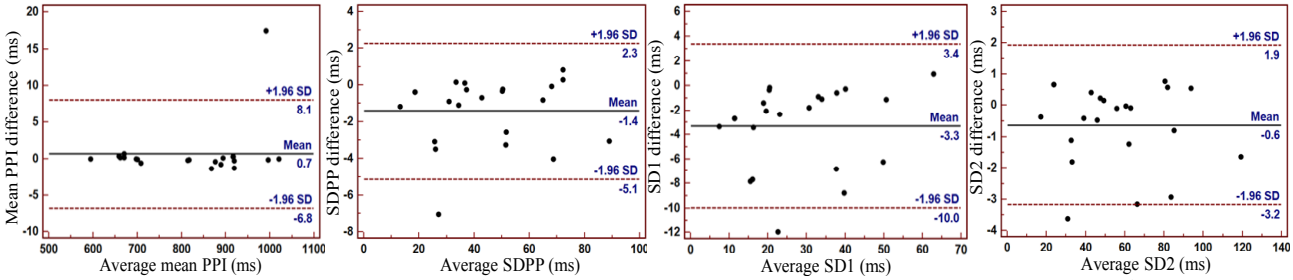

Figure 5. Bland-Altman plot was applied in agreement analysis between CPPG and NRPPG for four representative parameters: (a) Mean PPI, (b) SDPP, (c) SD1 and (d) SD2, which reflect cardio-physiological phenomena. (solid lines: the mean value of differences, broken lines: the upper and lower limits of agreement, i.e. the mean value of differences ± 1.96SD, SD: standard deviation).

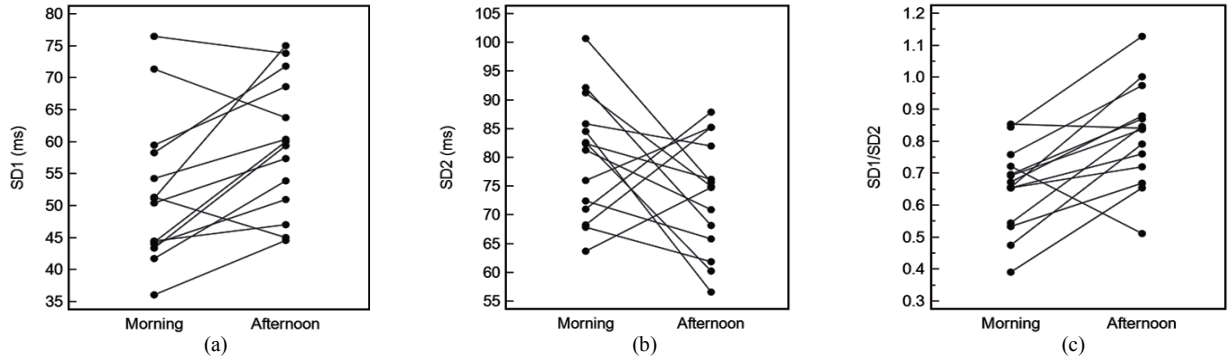

Figure 6. Illustrated individuals: (a) SD1, (b) SD2 and (c) their ratio SD1/SD2 from the physiological monitoring.

Table 3. SD1, SD2 and SD1/SD2 derived from PPG signals collected in the morning and afternoon.

Parameters	Morning	Afternoon	*p*
SD1 (ms)	51.9 ± 11.4	59.4 ± 10.4	0.0074
SD2 (ms)	80.0 ± 10.7	73.3 ± 9.9	0.1280
SD1/SD2	0.65 ± 0.13	0.82 ± 0.16	0.0011

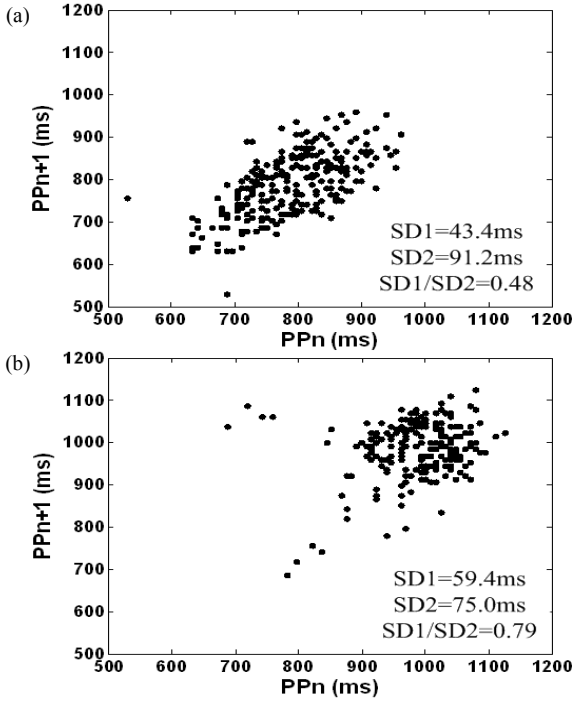

Figure 7. Representative Poincaré plots demonstrated cardio-physiological variations in (a) the morning and (b) the afternoon in the same day.

4. Discussion

4.1 Geometrical parameters for non-contact reflection PPG photonics engineering setup

Direct coupling is the phenomenon where the photodetector detects light directly from the light source while the light is not interacted with the tissue. This occurs when light is illuminated directly onto the photodetector, or when the photodetector is exposed directly to ambient light, which is usually a result of inappropriate probe selection or positioning [16]. Direct coupling is not negligible in non-contact PPG as light could be illuminated directly from the light source to the photodetector, depending on the positions of the light source, the photodetector and the tissue. However, the engineering model has considered this in the experiment to obtain a clear PPG signal.

In the NRPPG setup, the geometrical parameters, i.e. θ_{PL} and d_{PL}, were consolidated in the physical experiment to achieve a better performance. In the engineering setup, the light source and the photodetector are placed on the same side of the skin surface. The geometrical consideration in a such reflection PPG sensor is to determine the optimal distance between the light source and the photodetector. In the existing literature [17], there are two techniques that can enhance the quality of the plethysmogram: large light source driving current utilization and closer placement of photodetector to light source. The technique used in non-contact measurement not only considered the above principles but also the combination of the incident angle θ_{PL} and the distance d_{PL}, because these two geometrical parameters are to decide the optimal range which

determines the quality of PPG signal captured in the setup. The present sensor configuration in this study allowed us to primarily examine the banana effect on its shape and the length (l) as well as the distance d_{PL} between the VCSEL and the photodiode in the non-contact reflection measurement.

As detailed, the range of d_{PH} between 30-110 mm was determined as the largest optimal range when θ_{PL} was at the angle of 25° and d_{PL} was 25 mm. In the optimal range, the quality of the PPG signals is determined by (1) the illumination area with banana effect, and (2) the output power of light from the VCSEL to the illuminated tissue. The NRPPG sensor consists of the light emitter and the photodetector, and therefore measures the light that is scattered and reflected back to the surface of the skin. It has been identified theoretically and experimentally [10,18] that the backscattered light on the tissue surface is most likely to travel along a curved "banana-shaped" path through the tissue, and the depth and the length of the path are proportional to the distance between the light source and the detector. The length of the path cannot be precisely measured. Though the exact length is unlikely measureable, the actual path of the light was determined by the effect of the sensor location, as shown in Figure 2 and Table 1. The average depth that the light travels into tissue is approximately one-half the distance between the points of light incidence and transmittance on the sensor. In our study, the experimental results suggest that the length of banana-shaped curve determines the quality of PPG signals. Also, the banana effect on the optimal range was from 6 mm to 26 mm, which is consistent with a previous work [18], where the light propagation in a model of the adult head was examined in a similar situation. Additionally, the light illuminating the tissue should be strong enough to be detected by the photodiode since the output power of the VCSEL decreases with increasing distance d_{PL}.

4.2 Comparison of PPG signals between NRPPG and CPPG

In order to achieve a practical utilization, the NRPPG needs to cross-examine the main functions of the available photoplethysmographic devices. In the reality of NRPPG application, measuring heart activity and displaying a plethysmogram were targeted as the priority in this study. The comparison between "gold standard" and NRPPG seems useful and important to recognize both performances of these two techniques in a good agreement with Bland-Altman plot regardless of the operation conditions. We have presented the comparison results in this study between NRPPG and CPPG with respect to their primary functions of PPG by means of graphical and numerical analysis methods. The correlation coefficients were close to 1, and the errors between CPPG and NRPPG from Bland-Altman plots were distributed within the reasonable ranges. The good agreement for the heart rate indices indicates that NRPPG is compatible with CPPG.

4.3 Physiological monitoring

The results from the physiological monitoring experiment demonstrate that the NRPPG has a potential in physiological assessment. The quantitative Poincaré plot from the NRPPG signal revealed the short-term beat-to-beat variance of the PPI (SD1), the long-term beat-to-beat variance of the PPI (SD2) and their balance (SDl/SD2). The expending scatter due to the enhanced sympathetic activity in the afternoon (Figure 7) can be observed in the Poincaré plots, which is consistent with the explanations in the work from Tulppo et al. [13], where it was reported that SD2 decreased and SDl/SD2 ratio increased during exercise after a complete parasympathetic blockade. The experiment in our study suggests that sympathetic activation in the afternoon results in progressive reduction in the long-term oscillation of heart rate.

4.4 Motion artifact

Classes of signal corruption known as motion artifact are the primary sources of unwanted dynamics; so named because they originate from the consequences of voluntary or involuntary subject movement. Motion artifact encompasses corruption of PPG signals due to mechanical forces giving rise to change in: (1) the optical coupling between probe and subject, (2) physiology of the subject, (3) optical properties of the tissue due to geometric realignment, and (4) complex combination of all these effects. It is suggested that progress in understanding the origin and interpretation of PPG signals may be greatly improved by formulating a realistic physical model incorporating the major classes of artifact [4]. In this way, desired signal components could be separated from artifact by using information obtained from the physical model to equalize the distortion. Peter and Hayes [8] investigated the possibility of reducing artifact corruption of photoplethysmographic signals in real time, using an electronic processing methodology based on inversion of a physical artifact model. It has been shown that this methodology is successful in removing or reducing a large number of artifacts encountered in clinically relevant situations. In this study, the measurements were usually taken during a short period of time and the signals captured were controllably optimized, thus the motion artifact was minimized in the designated protocol.

5. Conclusion

A proof of concept for NRPPG with the photonics engineering model was created to achieve sophisticated and dynamic measurement in this study. The NRPPG photonics engineering setup adopted a VCSEL as the light source and a high-speed PiN photodiode as the photodetector to exhibit a good performance of the PPG signal capture in a proper geometrical arrangement. The agreement analysis shows the compatibility of the techniques between NRPPG and CPPG for the evaluation of heart activity. The physiological monitoring experiment proves the feasibility of physiological assessment when using the NRPPG technique. The outcome from the photonics engineering setup, the comparison study and the physiological monitoring experiment proves NRPPG's potential for remote monitoring.

Clearly, a remote PPG probe could be very useful for front-line clinicians to comfortably and confidently cope with situations such as patients with burned or healing skin, and

neonate monitoring against infection disease development. The applications from bench to bedside need more engineering efforts, such as increasing dynamic measurement range, improvement of signal-to-noise ratio and reduction of motion artifact. Specific requirements would be considered to achieve a higher level of clinical monitoring and physiological assessment.

Acknowledgements

The authors would like to acknowledge Loughborough University and Shanghai Jiao Tong University for supporting this joint research. The authors also would like to give special thanks to the volunteers who has participated in this study.

References

[1] A. B. Hertzman and C. R. Spealman, "Observations on the finger volume pulse recorded photoelectrically," *Am. J. Physiol. Meas.*, 119: 334-335, 1937.

[2] M. Nitzan, A. Babchenko, B. Khanokh and D. Landau, "The variability of the photoplethysmographic signal: a potential method for the evaluation of the autonomic nervous system," *Physiol. Meas.*, 19: 93-102, 1998.

[3] A. A. Kamal, J. B. Harness, G. Irving and A. J. Mearns, "Skin photoplethysmography: a review," *Comput. Methods Programs Biomed.*, 28,: 257-269, 1989.

[4] M. Hayes, "Artefact reduction in photoplethysmography," *Doctoral Thesis*, Loughborough University, Leicestershire, United Kingdom, 1998.

[5] P. Y. S. Cheang, "Feasibility of non-contact photoplethysmography," *Doctoral Thesis*, Loughborough University, Leicestershire, United Kingdom, 2008.

[6] S. Hu, J. Zheng, V. Chouliaras and R. Summers, "Feasibility of imaging photoplethysmography," *Proc. Int. Conf. on BioMedical Engineering and Informatics*, 72-75, 2008.

[7] F. P. Wieringa, F. Mastik and A. F. van der Steen, "Contactless multiple wavelength photoplethysmographic imaging: a first step toward "SpO2 camera" technology," *Ann. Biomed. Eng.*, 33: 1034-1041, 2005.

[8] P. R. Smith and M. J. Hayes, "Artifact reduction in Photoplethysmography," International Patent, WO/1999/032030, 1999.

[9] Y. Mendelson, "Pulse oximetry: theory and applications for noninvasive monitoring," *Clin. Chem.*, 38: 1601-1607, 1992.

[10] S. Feng, F. Zeng, and B. Chance, "Photon migration in the presence of a single defect: a perturbation analysis," *App. Opt.*, 34: 3826-3837 1995.

[11] J. Allen, "Photoplethysmography and its application in clinical physiological measurement," *Physiol. Meas.*, 28: R1-39, 2007.

[12] S. K. Mitra (Ed.), *Digital Signal Processing: A Computer-based Approach*, New York: McGraw Hill Companies, 1998.

[13] M. P. Tulppo, T. H. Makikallio, T. E. Takala, T. Seppanen and H. V. Huikuri, "Quantitative beat-to-beat analysis of heart rate dynamics during exercise," *Am. J. Physiol.*, 271: H244-252, 1996.

[14] J. M. Bland and D. G. Altman, "Statistical method for assessing agreement between two methods of clinical measurement," *Lancet*, 1: 307-310, 1986.

[15] J. M. Bland and D. G. Altman, "Measuring agreement in method comparison studies," *Stat. Methods Med. Res.*, 8: 135-60, 1999.

[16] S. J. Barker, J. Hyatt, N. K. Shah, and Y. J. Kao, "The effect of sensor malpositioning on pulse oximeter accuracy during hypoxemia," *Anesthesiology*, 79: 248-254, 1993.

[17] J. G. Webster (Ed.), *Design of Pulse Oximeters*, Bristol, UK: Institute of Physics Publishing, 1997.

[18] E. Okada, M. Firbank, M. Schweiger, S. R. Arridge, M. Cope, and D. T. Delpy, "Theoretical and experimental investigation of near-infrared light propagation in a model of the adult head," *Appl. Opt.*, 36: 21-31, 1997.